

PIOTR HOLNICKI\*, ANTONI ŻOCHOWSKI\*,  
KRZYSZTOF ABERT\*\* , KATARZYNA JUDA-REZLER\*\*

## FORECASTING OF SULFUR DEPOSITION ON A REGIONAL SCALE

The paper presents an algorithm for the prediction of sulfur deposition on a regional scale. The method is based on a dynamic, single-layer model of air pollution dispersion. The set of two transport equations, for the primary ( $\text{SO}_2$ ) and secondary ( $\text{SO}_4^{2-}$ ) sulfur species, is solved. Finally, the model generates spatial characteristics of the cumulated sulfur deposition due to transport and deposition processes, taking into account aerodynamical parameters of the terrain and chemical transformations.

The model is aimed at evaluating sulfur deposition originating from the major emission sources, representing the sector of energy generation. The emission intensity of each source and the time sequence of meteorological parameters within the period of simulation constitute the main input data. The model computes the contribution of each source to sulfur deposition over the predescribed time interval. The resulting total deposition map is a sum of the individual contributions. The land-cover characteristics is an important factor in this calculation.

Test computations were performed for the set of major power plants in Poland, using two estimation methods of dry deposition velocity for  $\text{SO}_2$ : (i) the standard literature value and (ii) the variable value calculated due to the modified version of RIVM's dry deposition model [2]. The results being presented refer to seasonal winter and summer depositions as well as to the total annual value.

### 1. THE TRANSPORT MODEL FORMULATION

The process of computing deposition forecast utilizes the discrete in time procedure, which simulates dynamics of air pollution dispersion. The basic input data contain emission intensity of each source (constant over a season) and time-variable meteorological parameters. The latter are entered as a sequence of the measurement data for each time step. Calculations performed in each time intervals consist of two basic stages:

- evaluation of  $\text{SO}_2$  and  $\text{SO}_4^{2-}$  concentrations,

---

\* Systems Research Institute, Polish Academy of Sciences, Warsaw.

\*\* Warsaw University of Technology, Institute of Environmental Engineering Systems, Warsaw.

- evaluation of total deposition resulting from the current concentration, meteorological data and the land-cover characteristics.

Concentrations forecasts of the main pollution components are generated by a single-layer dispersion model, based on the transport equations [5]. The model is of Lagrangian type and the computational technique is based on the method of characteristics. The mass balance of pollutants is calculated in each grid element for air parcels following the wind trajectories. The approach is source-oriented, thus the trajectory, which starts at the specific emission source, is observed until the mass of the parcel drops below 1% of its initial value or the parcel leaves the computational area. The procedure is applied in turn to all the individual sources, and the resulting concentrations are summed up to give the total concentration map in the current time step. Furthermore, the sulfur deposition in the consecutive time steps is calculated as a function of the current concentration, meteorological conditions and physical deposition parameters.

For computational purposes, the problem is formulated as a discrete in time with homogeneous spatial resolution of the domain. The uniform space discretization step will be denoted by  $h = \Delta x = \Delta y$ . Points along the trajectory are determined at discrete time moments based on the interval  $\tau$ , which in our computation was taken 15 min. The main output of the first stage of simulation constitutes the primary ( $\text{SO}_2$ ) and secondary ( $\text{SO}_4^{2-}$ ) concentrations, averaged over the discretization element and the mixing layer height. They finally yield deposition contribution in the consecutive time steps.

The initial concentrations depend on the emission intensity of a specific source and are calculated according to the formulae

$$q_1 = \frac{(1 - \beta)E\tau}{HM \cdot h^2}, \quad (1)$$

$$q_2 = \frac{\beta E\tau}{HM \cdot h^2}, \quad (2)$$

where  $q_1, q_2$  denote concentrations of  $\text{SO}_2$  and  $\text{SO}_4^{2-}$  [ $\mu\text{g} \cdot \text{m}^{-3}$ ],  $E$  is the total sulfur of this source [ $\text{g} \cdot \text{s}^{-1}$ ],  $\beta$  – fraction emitted directly as  $\text{SO}_4^{2-}$ ,  $HM$  – the mixing layer height [m].

The continuity equations for both components reflect spatial and temporal transformations of this initial value. They include advective transport, chemical transformations  $\text{SO}_2 \Rightarrow \text{SO}_4^{2-}$ , dry deposition and scavenging by precipitation.

$$\frac{\partial q_1}{\partial t} + \mathbf{w}\nabla q_1 + (k_{d_1} + k_{w_1})q_1 + k_t q_1 = 0, \quad (3)$$

$$\frac{\partial q_2}{\partial t} + \mathbf{w} \nabla q_2 + (k_{d_2} + k_{w_2})q_2 = k_t q_1, \quad (4)$$

where:

$k_{d_i}$  – dry deposition coefficient [ $s^{-1}$ ],

$k_{w_i}$  – coefficient of wet deposition due to scavenging by precipitation [ $s^{-1}$ ],

$k_t$  – coefficient of chemical transformation  $SO_2 \Rightarrow SO_4^{2-}$  [ $s^{-1}$ ],

$\mathbf{w} = [u, v]$  – wind velocity vector [ $m \cdot s^{-1}$ ].

The emission term does not appear on the right-hand side of (3) and (4), since the model simulates dispersion and environmental impact (spatial and temporal) of the concentrations (1) and (2), related to a source.

The transition from  $q_i(t)$  to  $q_i(t + \tau)$ ,  $i = 1, 2$ , is split into two steps, representing: i) advective transport using trajectory following technique, ii) changes of concentrations of pollutants in the air due to chemical transformations and deposition. The second step may be performed analytically. Assuming the coefficients in (3), (4) constant over the interval  $[t, t + \tau]$ , one can express the respective solutions in the following form (compare [6])

$$q_1(t + \tau) = q_1(t) \exp(-(k_{d_1} + k_{w_1} + k_t)\tau), \quad (5)$$

$$q_2(t + \tau) = \frac{k_t q_1(t)}{k_{d_2} + k_{w_2}} [1 - \exp(-(k_{d_2} + k_{w_2})\tau)] + q_2(t) \exp(-(k_{d_2} + k_{w_2})\tau). \quad (6)$$

The coefficients, which represent the decline due to dry and wet depositions in (3)–(6), are defined as follows:

$$k_{d_i} = \frac{v_{d_i}}{HM}, \quad k_{w_i} = \frac{\Lambda_i P}{HM} = \frac{w_{d_i}}{HM} \quad \text{for } i = 1, 2. \quad (7)$$

Here the dry deposition velocity  $v_{d_i}$  [ $m \cdot s^{-1}$ ] for  $SO_2$  can be preprocessed by two alternative methods. The first one is based on a specialized RIVM's algorithm [1], [2], [8] modified at the Institute of Environmental Engineering Systems (Warsaw Institute of Technology). The input data of this algorithm, discussed in Section 2 in more detail, consist of the meteorological forecast and physical parameters of the domain, e.g. the land-cover characteristics. An alternative method utilizes the constant value  $v_{d_1} = 0.008$  [ $m \cdot s^{-1}$ ]. In Section 4, the results of case study for these two approaches are compared. Utilizing the parametrization presented by SANDNES [6], dry deposition velocity for  $SO_4^{2-}$  is assumed  $v_{d_2} = 0.2v_{d_1}$  in both approaches.

The parameter  $P$  in the wet deposition formula denotes the precipitation height (in mm) accumulated over the time interval. According to SANDNES [6], the scavenging factor  $\Lambda_i$  reflects seasonal fluctuations in the air temperature. Details of the respective parameterization can be found in [4].

The concentrations  $q_1$  and  $q_2$  of  $\text{SO}_2$  and  $\text{SO}_4^{2-}$  constitute the output from the first stage of the model. The concentrations averaged over time-step are then used to calculate depositions in the consecutive steps of the algorithm. For the primary and secondary types of pollutants they are as follows:

$$D_i = (v_{d_i} + w_{d_i}) \cdot q_i \cdot \tau \quad \text{for } i = 1, 2. \quad (8)$$

Finally, the contributions of the consecutive time steps are summed up to give the total sulfur deposition over the interval of simulation.

The wind field in the computational region within the time interval of the forecast is the basic meteorological input utilized in the procedure of the pollutants transport simulation. Due to the structure of the transport model, the wind preprocessor represents a single-layer approximation of the three-dimensional field. It also reflects the dynamics of temporal changes within the forecasting interval.

The aim of the respective module is to generate wind-field trajectories, which are next used in simulation of the pollutants transport. The approach applied is based on the spatial and temporal interpolation of the sequence of meteorological data obtained from selected measurement stations (compare figure 1). The field is preprocessed by the spatial interpolation of the input data measured (anemometric wind and geostrophical wind components), and time interpolation of the consecutive episodes. A more detailed description of the wind submodel can be found in [4].

The other meteorological fields (precipitation, relative humidity, temperature) are approximated by time-variable and stepwise in space functions.

## 2. MODEL OF DRY DEPOSITION

In order to improve the predictions of the transport model, the detailed dry deposition submodel has been used. The  $\text{SO}_2$  concentrations strongly depend on dry deposition process, so its parameterization is essential for the model results. The dry deposition submodel for sulfur species, based on the original multi-species RIVM's (National Institute of Public Health and Environmental Protection, Bilthoven, the Netherlands) dry deposition model [2], [8], has been developed and tested. The original RIVM's model, named DEPAC, considers seven sulfur and nitrogen species. For the purposes of current work only the part dealing with sulfur dioxide has been extracted. Model sensitivity to its input parameters has been extensively tested. Analysis of test results allowed us to neglect some input parameters. The modified version of the  $\text{SO}_2$  dry deposition submodel has been integrated with sulfur air pollution trajectory model discussed in the previous sections.

The dry deposition velocity  $v_d$  represents the ability of the given land cover to absorb given pollutant under specific meteorological conditions. Adequate parameterization of  $v_d$  is very important as both concentration and deposition values depend on that value. For the majority of pollutants  $v_d$  strongly varies in time and space.

Dry deposition of atmospheric gases on the ground comprises three stages: the first, the material must be transported through the atmosphere to the receptor surface (turbulent layer); the second, there occurs a transport through the quasi-laminar layer at the surface; the last, the gas must be captured by the surface [10], [1]. Thus, to account for these three stages of deposition process, the parameterization of  $v_d$  in the dry deposition model is based on the resistance analogy:

$$v_d(z) = \frac{1}{R_a(z) + R_b + R_c}, \quad (9)$$

where:

- $v_d(z)$  – dry deposition velocity at the height  $z$  [ $\text{m} \cdot \text{s}^{-1}$ ],
- $R_a$  – aerodynamic resistance at the height  $z$  [ $\text{s} \cdot \text{m}^{-1}$ ],
- $R_b$  – laminar layer resistance [ $\text{s} \cdot \text{m}^{-1}$ ],
- $R_c$  – surface resistance [ $\text{s} \cdot \text{m}^{-1}$ ].

The  $R_a$  value depends mainly on the atmospheric turbulence intensity – the higher the turbulence, the more intensive transport to the surface. The atmospheric resistance to transport of gasses across the constant flux layer is assumed to be similar to that of heat [1]:

$$R_a(z) = \frac{1}{k \cdot u_*} \left[ \ln\left(\frac{z}{z_0}\right) - \Psi_h\left(\frac{z}{L}\right) + \Psi_h\left(\frac{z_0}{L}\right) \right], \quad (10)$$

where:

- $k$  – von Karman constant,
- $u_*$  – friction velocity [ $\text{m} \cdot \text{s}^{-1}$ ],
- $z_0$  – aerodynamical roughness coefficient [m],
- $L$  – the Monin–Obukhov length [m],
- $\Psi_h$  – integrated stability function for heat.

Integrated stability function for the heat  $\Psi_h$  is calculated as follows (ERISMAN [1]):

$$\Psi_h\left(\frac{z}{L}\right) = -5.2 \left(\frac{z}{L}\right) \quad \text{for } L > 0 \quad (11)$$

and

$$\Psi_h\left(\frac{z}{L}\right) = 2 \cdot \ln\left(\frac{1+x^2}{2}\right) \quad \text{for } L < 0, \quad (12)$$

where:

$$x = \left[ 1 - 16 \frac{z}{L} \right]^{1/4}.$$

In the sublaminal layer, pollutant transport to the surface depends on both turbulence and molecular diffusion of the pollutant and can be approximated as [1]

$$R_b = \frac{2}{k \cdot u_*} \left( \frac{Sc}{Pr} \right)^{2/3}, \quad (13)$$

where:

$Sc$  – Schmidt number;  $Sc = \nu/D$ , where  $\nu$  is the kinematic viscosity of air ( $0.15 \text{ cm}^2 \cdot \text{s}^{-1}$ ),

$D$  – the molecular diffusivity of the pollutant [ $\text{cm}^2 \cdot \text{s}^{-1}$ ],

$Pr$  – Prandtl number;  $Pr = 0.72$ .

On the surface the absorption of the pollutant is dependent on the characteristics of both component and receptor.  $R_c$  is the function of chemical, biological and physical characteristics of the receptor, chemical and physical characteristics of pollutant as well as time of the year and time of the day. The value  $R_c$  is the most difficult to parameterize. In the RIVM's scheme, the measurement of dry deposition taken during EUROTRAC and BIATEX experiments (see [2] and [7]) have been used for  $R_c$  parameterization. Procedures applied in the dry deposition model are based on the Monin–Obukhov theory for surface layer. As in transport model the stability is determined by Pasquill's stability classes, for the determination of the Monin–Obukhov length ( $L$ ) Golder's graphical relationships connecting the stability parameters have been applied. The friction velocity  $u_*$  has been calculated according to the logarithmic profile [5]

$$u_* = k u_a \cdot \left[ \ln \left( \frac{z_a}{z_0} \right) \right]^{-1}, \quad (14)$$

where:

$u_a$  – anemometric wind velocity [ $\text{m} \cdot \text{s}^{-1}$ ],

$z_a$  – anemometric height [m].

Aerodynamical roughness coefficients  $z_0$  have been obtained for computational grid with the resolution of  $10 \text{ km} \times 10 \text{ km}$ . Annual mean values of  $z_0$  have been calculated from the data taken from ECMWF (European Centre for Medium-Range Weather Forecast Reading, UK).

The land-cover data for Poland are essential – in each computational grid, they are needed as an input to the dry deposition submodel. The land-cover map for the territory of Poland in the adopted computational grid has been prepared on the basis of RIVM's original data (compare [9]) with geographical resolution  $10' \times 10'$ . A geographical information system (Arc/Info) was used to convert original data into a projection and resolution suitable for the adopted computational grid (resolution  $10 \text{ km} \times 10 \text{ km}$ ). The following land-use categories are included in original data: coniferous and mixed forest, deciduous forest, permanent crops, grassland, urban areas, arable

land, inland water, sea and "other". An additional category, i.e. "high mountain forest", has been added to the land-cover characteristics in the current work.

Calculations of the value  $v_d$  have been carried out by means of dry deposition model described above. As a result, the SO<sub>2</sub> dry deposition velocity map at each node of the computational grid has been obtained, constituting an input into the transport model calculations discussed in section 1. In the next section, the results of test computations are presented. They show, how two various methods of dry deposition simulation (constant, literature value of  $v_d$  and RIVM algorithm) affect the final deposition map.

### 3. SIMULATION OF SULFUR DEPOSITION IN POLAND

The model has been applied in generating seasonal and annual sulfur deposition resulting from the major power and heating plants of the Polish energy sector. The computational domains is based on EMEP-oriented rectangle, 900 km × 750 km, containing Poland (compare figure 1). The uniform space resolution, based on the element of size 10 km × 10 km, is applied, thus the dimension of computational grid is 90 × 75. The set of 91 dominating sources has been taken into account. Season-averaged emissions of the major sources are presented in an aggregated form in the table.

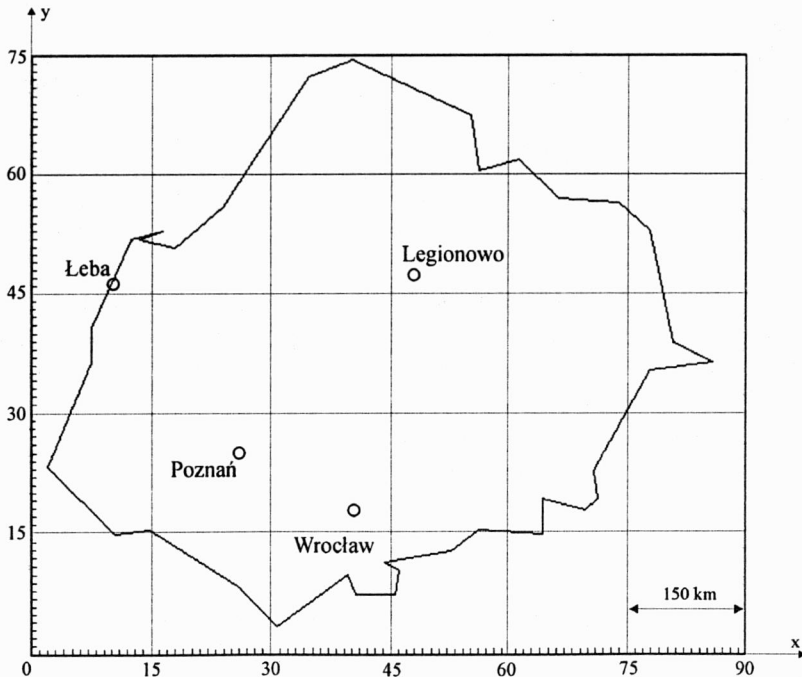


Fig. 1. Poland in EMEP coordinates and the main aerological measurement stations

Table

Aggregated emission characteristics of the major sources (data from the year 1996)

Power plant	No. of stacks	Grid element (x, y)-coord.	Range of stack heights [m]	SO <sub>2</sub> emission - winter [Mg · h <sup>-1</sup> ]	SO <sub>2</sub> emission - summer [Mg · h <sup>-1</sup> ]
Adamów	2	(31.6, 5.6)	150	1.9424	1.0251
Bełchatów	3	(48.2, 32.1)	300	30.7043	19.8995
Bydgoszcz	3	(27.4, 38.8)	73-100	3.3046	0.4915
Chorzów	2	(40.5, 18.4)	100-180	1.6023	0.1940
Dolna Odra	2	(9.7, 22.1)	250	9.4608	4.9932
Gdańsk	3	(45.8, 36.2)	120-200	2.8193	0.3845
Gdynia	2	(45.6, 36.6)	85-150	1.9769	0.4185
Jaworzno	2	(58.7, 24.7)	120-300	5.7122	3.2146
Konin	4	(31.6, 5.6)	100-120	4.6431	2.9376
Kozienice	3	(55.7, 47.4)	200-300	8.5628	4.5192
Kraków	2	(63.8, 27.0)	225-260	4.5560	0.9257
Łągisza	2	(57.5, 24.7)	160-200	4.7152	2.4885
Łaziska	2	(57.7, 21.0)	160-200	5.4685	3.0322
Łódź	6	(46.2, 57.9)	50-200	8.4557	1.3328
Ostrołęka	2	(42.6, 57.8)	120-250	4.7678	2.0003
Pątnów	2	(35.5, 34.0)	150	15.6949	9.3085
Połaniec	2	(66.2, 38.3)	250	12.1660	6.4210
Rybnik	2	(55.7, 19.5)	260-300	8.3418	4.4112
Siekierki	2	(48.8, 49.0)	120-200	6.8124	1.0926
Siersza	2	(60.3, 25.3)	150-260	3.8595	2.0369
Skawina	2	(63.6, 25.7)	120	3.2744	1.7281
Turów	3	(31.6, 5.6)	150	17.8486	10.3945
Wrocław	2	(40.5, 18.4)	120-180	3.6988	0.5794
Zabrze	2	(40.5, 18.4)	100-180	2.2615	0.3868
Żerań	3	(47.6, 49.2)	100-200	3.2003	0.4876

The input into the wind field submodel is based on the spatial and temporal interpolation of the meteorological data from four aerological measurement sites: Poznań, Wrocław, Łeba and Legionowo, as shown in figure 1. Each station records every 12 hours the following set of data:

- components of the anemometric wind  $u_A, v_A$ ,
- components of the geostrophic wind (850 hPa)  $u_G, v_G$ ,
- precipitation intensity,
- temperature,
- relative humidity.

The above data have to be spatially and temporarily interpolated over the computational domain, according to the procedure discussed in [4] in more detail. The wind field, in this case, is preprocessed by the spatial interpolation of the measured input data of four stations, and temporal interpolation of the consecutive sets of data.



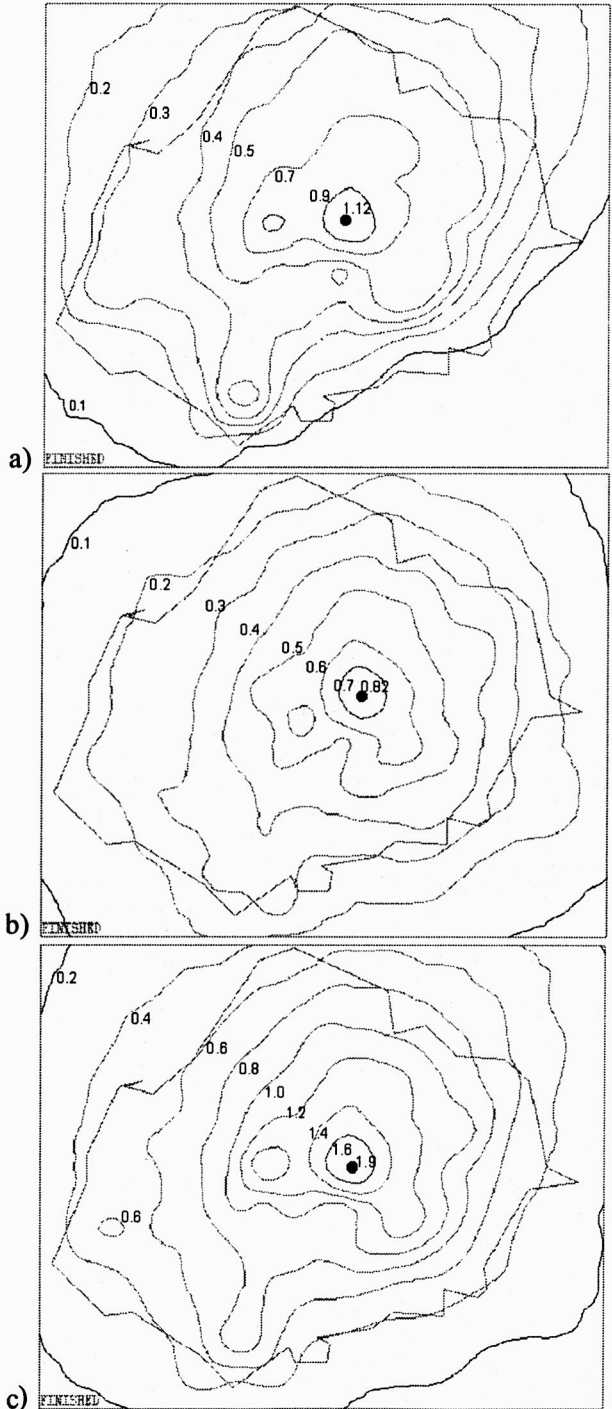
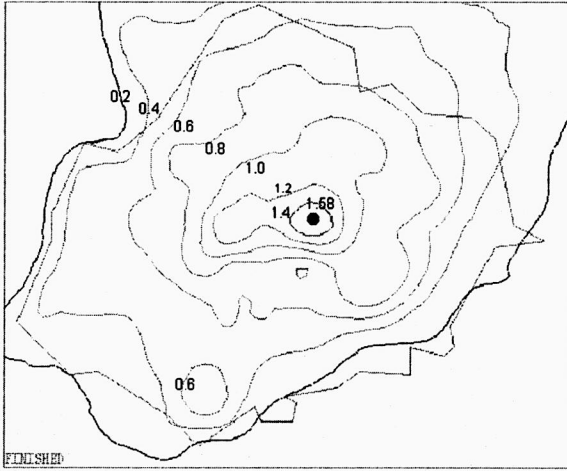
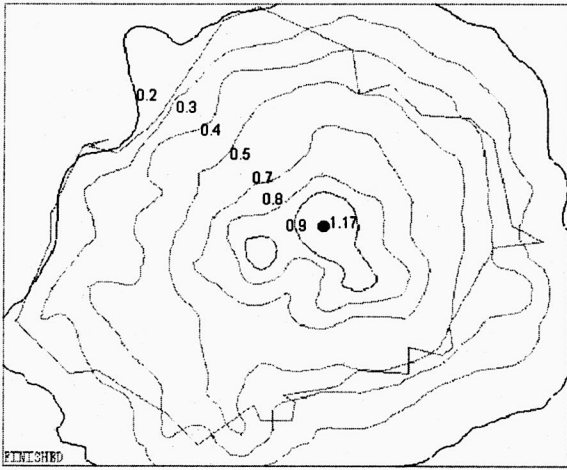


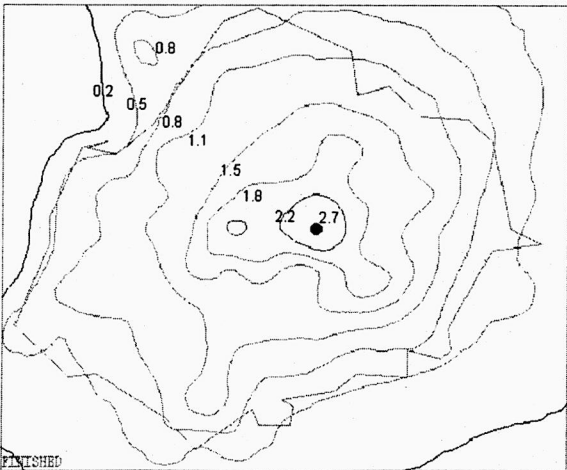
Fig. 2. Total sulfur deposition in 1996 [ $\text{gS} \cdot \text{m}^{-2}$ ] for constant  $v_d = 0.008 \text{ m} \cdot \text{s}^{-1}$ ;  
 a) winter season, b) summer season,  
 c) annual



a)



b)



c)

Fig. 3. Total sulfur deposition in 1996 [ $\text{gS} \cdot \text{m}^{-2}$ ] for RIVM dry deposition model; a) winter season, b) summer season, c) annual

The assumed linearity of the dispersion process (linear dependence of the concentration on the emission intensity of the source) allows us to simulate separately the environmental impact of all the sources under consideration. Then, the total deposition map can be calculated as a superposition of those individual contributions.

Results of computation shown in figures 2–3 present sulfur deposition maps obtained for two methods of dry deposition parameterization. The first one is related to constant value of dry deposition velocity,  $v_d = 0.008 \text{ [m} \cdot \text{s}^{-1}\text{]}$ . The other map presents results obtained for variable (in space and time) dry deposition velocity computed by the built-in RIVM procedure discussed in section 2. As one can see, the maximum deposition values near the domain sources are substantially higher when variable deposition velocity is applied.

#### 4. CONCLUSIONS

The parameterization of dry deposition velocity  $v_d$  is very important in air dispersion models, as both concentration and deposition values strongly depend on that factor. For this purpose, to improve predictions of the transport model, the specialized dry deposition submodel has been built in and analyzed. The dry deposition submodel for sulfur species has been developed and tested based on the original multi-species RIVM's (the National Institute of Public Health and Environmental Protection, Bilthoven, the Netherlands) dry deposition model [7].

It is known and confirmed by the maps presented that the sulfur deposition in Poland is rather high. It should be mentioned that the total (from all sources) sulfur emission in Poland in the years 1985–1997 has been reduced almost twice (from 4300 Gg of  $\text{SO}_2$  in 1985 to 2181 Gg of  $\text{SO}_2$  in 1997). Nevertheless, the emission is still substantial on the European scale, and the resulting deposition is still higher than the critical loads for sulfur. The total (dry + wet) sulfur deposition for the whole country, related to the 91 emission sources analyzed, equals 390 Gg (S) when using constant value of dry deposition velocity (figure 2) and 535 Gg (S) when using RIVM's dry deposition model for calculating variable in time and space dry deposition velocities (figure 3).

Thus, the total annual sulfur deposition for Poland calculated by using dry deposition model is by about 27% higher than the deposition calculated by using constant value of  $v_d$ . Taking into account the seasonal distributions of total deposition in Poland we can state that in both calculations, the values for the winter season are higher than those for the summer season. This is strictly related to the annual distribution of emission – in the winter (the so-called “heating season”) emissions from the majority of power stations are almost twice as high as those of the summer season.

The built-in dry deposition model (figure 3) generates higher values of deposition, especially in the neighbourhoods of the major emission sources. One can distinguish the following areas of external total annual values: the surroundings of the Bełchatów elec-

tric power station – central part of Poland, with the maximum deposition of  $1.9\text{--}2.7 \text{ g(S)} \cdot \text{m}^{-2} \cdot \text{yr}^{-1}$  and the surroundings of the Turów electric power station (the border of Poland, the Czech Republic and Germany, region of the Karkonosze mountains) with the maximum deposition of  $0.9\text{--}1.4 \text{ g(S)} \cdot \text{m}^{-2} \cdot \text{yr}^{-1}$ . The respectively higher deposition values are related to variable  $v_d$  case (compare figure 2 and figure 3).

There are also differences in the resulting spatial distributions of sulfur deposition in both algorithms. RIVM's model, for example, shows a remarkable influence of the Gdańsk power stations on the East Baltic region, while this effect is not indicated by the other approach. On the other hand, the lower deposition for the constant  $v_d$  case causes respectively higher concentrations of  $\text{SO}_2$  in regions of major sources location and higher impact on distant receptors.

It must be also stressed that the implementation of RIVM deposition algorithm causes a substantial increase of the computing time of the entire transport model (by about four times comparing to that of the constant  $v_d$  case), since additional computations have to be performed in all grid elements in the consecutive time steps. The computing time is not, however, a critical factor in the annual deposition analysis. On the other hand, the substantial differences between both results suggest that utilizing the variable dry deposition approach gives more realistic and accurate results, which is important for resulting accuracy of dispersion and deposition models.

#### ACKNOWLEDGEMENTS

Authors are grateful to Dr. J.W. Erisman and Dr. A. van Pul from RIVM (the National Institute of Public Health and Environmental Protection, Bilthoven, the Netherlands) for giving access to the source version of multi-species dry deposition model (DEPAC).

This research was partially supported by the ESPRIT Project 20288 Cooperation Research in Information Technology (CRIT2): "Evolutionary Real-time Optimization System for Ecological Power Control".

#### REFERENCES

- [1] ERISMAN J.W., *Atmospheric deposition of acidifying compounds in the Netherlands*, PhD-thesis, University of Utrecht, 1992, the Netherlands.
- [2] ERISMAN J.W., van PUL W.A.J., WYERS G.P., *Parameterization of surface resistance for the quantification of atmospheric deposition of acidifying pollutants and ozone*, *Atmospheric Environment*, 1994, 28, 2595–2607.
- [3] GOLDER D., *Relations among stability parameters in surface layer*, *Boundary Layer Meteorology*, 1972, 3, 47–58.
- [4] HOLNICKI P., ŻOCHOWSKI A., WARCHAŁOWSKI A., *Regional-scale air pollution dispersion model*, *Environment Protection Engineering*, 2001, 33, 133–145.
- [5] LYONS T.J., SCOTT W.D., *Principles of Air Pollution Meteorology*, Balhaven Press, London, 1990.
- [6] SANDNES H., *Calculated budgets for airborne acidifying components in Europe*, Report EMEP/MSC-W, 1/93, The Norwegian Meteorological Institute, Oslo, 1993.

- [7] SELAND Ø., van PUL A., SOTEBERG A., TOUVINEN J.-P., *Implementation of a Resistance Dry Deposition Module and Variable Local Correction Factor in the Lagrangian EMEP Model*, Report EMEP/MSC-W, 1995, 3/95, The Norwegian Meteorological Institute, Oslo.
- [8] Van PUL A., *Dry deposition model (FORTRAN code, DEPAC)*, Report LLO/RIVM, 1994, Bilthoven, the Netherlands.
- [9] VELDKAMP H., VAN de VELDE R., *Mapping Land Use and Land Cover for Environmental Monitoring on a European Scale*, [in:] *Calculation and mapping of critical threshold in Europe* (eds.: Posch M., de Smet P.A.M., Hettelingh J.-P. and Downing R.J.), CCE Status Report 1995, RIVM rep. 259101004, 1995, Bilthoven, the Netherlands, 51–60.
- [10] VOLDNER E.C., BARRIE L.A., SIROIS A., *A literature review of dry deposition of oxides of sulfur and nitrogen with emphasis on long-range transport modeling in North America*, Atmospheric Environment, 1986, 20, 2101–2133.

### PROGNOZOWANIE DEPOZYCJI SIARKI W SKALI REGIONALNEJ

Przedstawiono algorytm prognozowania depozycji siarki w skali regionalnej. W zastosowanej metodzie wykorzystano dynamiczny, jednowarstwowy model rozprzestrzeniania się zanieczyszczeń atmosferycznych, który opiera się na układzie równań transportu dla zanieczyszczeń pierwotnych ( $\text{SO}_2$ ) oraz wtórnych ( $\text{SO}_4^{2-}$ ). Na podstawie modelu opracowano mapy rozkładu przestrzennego skumulowanych wartości depozycji siarki w regionie, uwzględniające wpływ parametrów aerodynamicznych i przemian chemicznych na proces transportu zanieczyszczeń.

Model ma służyć do oceny wielkości depozycji związanej z oddziaływaniem głównych źródeł energetyki zawodowej. Podstawowymi danymi wejściowymi są intensywność źródła emisji oraz ciąg danych meteorologicznych dla przyjętego okresu symulacji. Ważnym czynnikiem brany pod uwagę w obliczeniach jest charakterystyka pokrycia terenu. Końcowe pole depozycji stanowi sumę udziałów poszczególnych źródeł.

Obliczenia testowe przeprowadzono dla grupy największych zakładów energetycznych w Polsce, wykorzystując dwa sposoby obliczania prędkości suchej depozycji  $\text{SO}_2$ : (i) standardową, stałą wartość literaturową oraz (ii) zmienną wartość  $v_d$ , obliczoną na podstawie zmodyfikowanej wersji modelu suchej depozycji RIVM [2]. Prezentowane wyniki przedstawiono jako mapy depozycji siarki dla lata, zimy oraz całego roku.

